ACS APPLIED POLYMER MATERIALS

pubs.acs.org/acsapm

Article

Stimuli-Responsive Luminescent Solar Concentrators Based on Photoreversible Polymeric Systems

Giovanni Fortunato, Elisavet Tatsi, Francesca Corsini, Stefano Turri, and Gianmarco Griffini*

Cite This: *ACS Appl. Polym. Mater.* 2020, 2, 3828−3839

Read Online

ACCESS | Metrics & More | Article Recommendations | Supporting Information

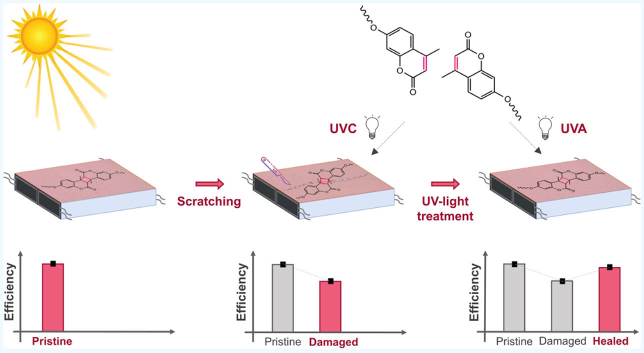

ABSTRACT: Luminescent solar concentrators (LSCs) consist of dye-doped, highly transparent, plastic plates aimed at improving the building integration and reducing the cost of photovoltaic (PV) technology. In the thin-film configuration, the surface of these devices is particularly exposed to mechanical damage and to a consequent loss of performance in terms of power conversion. To address this issue, the first demonstration of a healable thin-film LSC based on a photoreversible polymer network as the host matrix is presented in this work. The photoresponsive matrix is obtained by simple UV curing of a coumarin functional polyurethane through reversible [2+2] cycloaddition. The final cross-linked coating is optically clear and exhibits excellent scratch remendability after suitable UVC/UVA exposure. The LSC devices obtained by doping the responsive matrix with perylene- or coumarin-based organic dyes possess a remarkable PV performance, comparable with control devices based on poly(methyl methacrylate). The loss of performance induced by surface mechanical scratches can be fully recovered by UV irradiation, as a result of the photoreversibility of the coumarin functional polymer network. The healing strategy presented here, purely light-triggered, expands the tools for the design of durable and responsive thin-film LSCs.

KEYWORDS: *stimuli-responsive polymers, photohealable polymers, [2+2] cycloaddition, fluorescent coatings, luminescent solar concentrators*

1. INTRODUCTION

The growing shift toward renewable resources for energy production has recently raised again the interest in photovoltaic (PV) technologies. Their efficient integration into existing buildings is one of the key challenges to be faced to meet the growing global demand for electricity.[1] In this context, luminescent solar concentrators (LSCs) represent a practical solution to this issue, owing to their transparency, easy color and shape tunability, and direct production from available structural materials (typically glass or commodity polymers).[2−4] An LSC device is essentially made of a transparent material (i.e., the host matrix) doped with a luminescent species, or luminophore, able to harvest incident solar light by absorption. A fraction of the photons emitted by the luminophore (usually by fluorescence) remains trapped within the matrix, as the latter has a higher refractive index than the surrounding environment (air), and is conveyed toward the edges of the device and collected by small-area PV cells.[5] The whole photon collection process is not exempt from loss events, which strongly affect the performance of the device. In this context, an ideal luminophore should provide a broad light collection, possess a high luminescent quantum yield (LQY), and a large Stokes shift to minimize self-absorption.[6] To meet these demands, a wide variety of dopants, mainly organic dyes, inorganic quantum dots, and transition-metal complexes, have been developed in the last few decades.[7−10] The host matrix plays a crucial role as well since it should be highly transparent to minimize parasitic absorption, have a high refractive index (>1.5) and a homogeneous surface to avoid reflection and scattering phenomena, and should efficiently disperse the luminophore.[5] Conventional thermoplastics such as polyacrylates (in particular poly(methyl methacrylate), PMMA) and polycarbonates usually meet these requirements and thus represent a common and cheap choice for the design of LSC devices.[5,11]

A real-life implementation of these matrixes raises the issue of durability of such LSC devices in outdoor environment. In fact, weathering caused by environmental agents such as radiation, oxygen, moisture, dust, and mechanical damages can significantly degrade the polymer matrix, resulting in a reduction in the smoothness of device surface, a consequent

Received: May 15, 2020
Accepted: August 12, 2020
Published: August 12, 2020

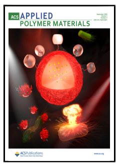

https://dx.doi.org/10.1021/acsapm.0c00515

loss of performance,[12,13] and, eventually, the failure of the coating.[14] In light of this, some strategies to overcome mechanical damages of LSCs during outdoor service life have recently been proposed. Among these, laminated LSCs, in which a covering glass is applied onto the LSC top surface, appear to be an interesting practical solution. Indeed, glass lamination not only avoids the mechanical scratching of the active layer but also protects it from direct exposure to the surrounding environment.[15−19] However, due to the decrease of the concentration factor, larger PV cells are typically required on the edges of the laminated LSCs, which might have an effect on the cost of generated electricity (€/kWh).[17] Also, a fraction of the incident light (mostly in the UV region) could be cut off from the covering glass, thus partly reducing the number of photons potentially harvested by the luminophore in that wavelength range. Alternatively, functional host matrixes are clearly advantageous over commodity plastics. For example, extended photochemical stability and self-cleaning ability were imparted to a LSC device by designing a functional host matrix based on cross-linked fluoropolymers doped with a perylene dye.[20,21] Within this context, the self-healing function could extend the lifetime of LSC devices, particularly those in thin-film configuration, which are more prone to mechanical damage with respect to bulk-configuration devices owing to their high surface/thickness ratio.[22]

Self-healing coatings are a class of smart coatings able to repair small mechanical damages autonomously (typically by the rupture of microcapsules containing the healing agent) or in response to a suitable stimulus in the form of heat or radiation (a nonautonomous mechanism).[23−27] Within this context, the radiation stimulus (visible or UV light) offers the possibility of temporal and spatial control of the healing process typically not easy with thermally induced healing.[28,29] UV-induced self-healing is based on the reversible dimerization via [2+2] cycloaddition of specific photoresponsive groups such as coumarin, cinnamoyl, anthracene, or thymine derivatives. Dimerization is achieved by irradiating the species in solution or in the solid state at $\lambda > 350$ nm, while upon irradiating the dimers at a lower wavelength (typically 254 nm), bond cleavage is favored.[30] Thus, a photoreversible polymer network can be obtained by incorporating in a linear chain photoresponsive groups acting as cross-linkers. Since the network has a reversible nature, the material increases its mobility during UVC irradiation and toughens again under UVA/visible light, allowing repair of damaged surfaces. In particular, coumarin derivatives, owing to the wide availability of their precursors and their easy functionalization, represent a convenient platform for the design of photoresponsive polymers[31] for applications in various fields, including resists in nanoimprint lithography,[32] controlled drug release,[33−35] and self-healing films or coatings.[36−47]

Based on these considerations, in this work, the first demonstration of a UV-triggered self-healing polymer for thin-film LSC applications is reported. A coumarin-functionalized macromer, obtained from a one-step modification of a polyisocyanate prepolymer, was cross-linked under UVA light to yield a highly transparent and colorless coating. Owing to its excellent photoreversibility, evaluated from absorption and fluorescence spectroscopies, the system was able to successfully heal upon mechanical damage, under a suitable UVC/UVA light irradiation cycle. Embedding the dimer-based matrix with a perylene or a coumarin derivative allowed to obtain LSC devices with efficiency comparable with reference state-of-the-art systems. Moreover, a purely photoinduced healing of the damaged surface of the device resulted in a complete recovery of the original performance.

2. EXPERIMENTAL SECTION

2.1. Materials. 7-Hydroxy-4-methylcoumarin (HMC), 2-bromoethanol, dibutyltin dilaurate (DBTDL), *N*,*N*-dimethylformamide (DMF), ethyl acetate, and chloroform were obtained from Sigma-Aldrich and used as received. Potassium carbonate was obtained from CARLO ERBA Reagents. Desmodur XP 2599 (DX2599, aliphatic isocyanate prepolymer with 6.0 wt % NCO, average functionality of 4.2) was kindly provided by Covestro. Lumogen F Red 305 (LR305) was supplied by BASF and Coumarin 6 (C6), more specifically 3-(2-benzothiazolyl)-7-(diethylamino) coumarin, by TCI Chemicals. PMMA (ALTUGLAS BS 550) and index matching liquid 150 (IML150) were purchased from Arkema and Norland, respectively. Monocrystalline high-efficiency silicon solar cells were provided by IXYS (IXOLAR SolarBIT KXOB22-12X1F, active area = 2.2 × 0.6 cm^2, $V_{OC} = 0.64 \pm 0.01$ V, $J_{SC} = 42.60 \pm 0.42$ mA cm^{-2}, FF = 69.4 ± 0.3%, power conversion efficiency (PCE) = 18.69 ± 0.23%).

2.2. Synthesis of 7-(Hydroxy ethoxy)-4-methylcoumarin (HEOMC). HEOMC was synthetized according to a reported procedure with some modifications.[17] Typically, HMC (8 g, 45.4 mmol) was dissolved in 50 mL of DMF in a round-bottom flask equipped with a magnetic stirrer. Upon addition of 2-bromoethanol (8.6 g, 68.8 mmol) and potassium carbonate (12.6 g, 91.2 mmol), the flask was sealed and placed under an inert atmosphere through evacuation-backfilling with nitrogen. The mixture was stirred for 18 h at 90 °C, cooled to room temperature, and poured into 150 mL of ice water. The solid was collected by filtration and recrystallized twice from ethyl acetate to give a yellow powder. Yield = 78%; mp 149 °C; IR (KBr): ν = 3439 (s; ν_s(O−H)), 3069 (w, ν_s(aromatic C−H)), 2955, 2931 (w, ν_s(aliphatic C−H)), 1701 (s, ν_s(C=O)), 1621 (s, ν_s(C=C pyrone ring)), 1555, 1388 (m, aromatic ν_s(C=C)) 1153, 1076 cm^{-1} (m, ν_s(C−O)). ^{1}H-NMR (400 MHz, DMSO-d_6, δ): 7.65 (m, 1H, Ar−H), 6.95 (m, 2H, Ar−H), 6.18 (d, J = 1.2 Hz, 1H, C=C−H), 4.92 (br, 1H, −OH), 4.09 (t, J = 4.9 Hz, 2H, $-CH_2-$), 3.73 (t, J = 4.9 Hz, 2H, $-CH_2-$), 2.38 (d, J = 1.1 Hz, 3H, $-CH_3$).

2.3. Synthesis of Coumarin Urethane Prepolymer (PU-Cou). Desmodur XP 2599 (7.3 g, 10.4 mmol of NCO) was weighed into a two-necked round-bottom flask equipped with a magnetic stirrer. The flask was sealed with a rubber septum and heated for 1 h at 70 °C, under dynamic vacuum, to dry the prepolymer. Upon cooling to rt, the flask was filled with nitrogen and a solution of HEOMC (2.30 g, 10.4 mmol) in 80 mL of chloroform was added. DBDTL (1 wt % with respect to dry reagents) was injected and stirring was continued for 2 h at room temperature (rt), under an inert atmosphere. The reaction was monitored by following the disappearance of 2270 cm^{-1} band (NCO stretching in isocyanates) in the FTIR spectra. The solvent was removed under vacuum and the residual solids were redissolved in THF (10 wt %). Insoluble particles (unreacted HEOMC) were separated by centrifugation, while the supernatant was dried in a vacuum oven (50 °C, 24 h) to give a waxy, white solid. Yield = 92%.

2.4. Coating Preparation and UV Irradiation. PU-Cou was spin-coated (600 rpm, 60 s) from chloroform solutions (120 mg/mL) on glass or quartz slides using a Laurell WS-400BZ-6NPP/LITE instrument. The obtained samples were irradiated under a UV polymerization apparatus (POLIMER 400W, Helios Quartz,) equipped with high-pressure mercury lamps. Specifically, cross-linking was performed using a UVA lamp (Zs type, Helios Quartz) with the emission window between 315 and 400 nm and with radiative power density equal to 54.6 mW/cm^2. De-cross-linking was performed under a UVC lamp (Zp type, Helios Quartz), with the emission window between 100 and 400 nm, equipped with a 254 nm bandpass filter (Omega Optical, 254 nm CWL, Hard Coated OD Bandpass Filter), and a power density of 2.4 mW/cm^2. Irradiations were performed both in air and an inert atmosphere (flux of nitrogen).

2.5. LSC Device Fabrication. LSCs were fabricated in thin-film configuration starting from chloroform solutions of PU-Cou macromer (120 mg/mL) with different concentrations of LR305 or C6 dyes (1−9 wt % with respect to dry polymer). Films with an average thickness of ∼1.5 μm were obtained by spin-coating (600 rpm for 60 s) onto 4.4 × 4.4 × 0.6 cm^3 glass slabs and UVA irradiation (120 min). LSCs were attached to two modules, each incorporating two monocrystalline silicon solar cells connected in series, by means of a low-viscosity IML150 index matching liquid (viscosity 100 cP, refractive index ∼1.52), so that two opposite edges of the glass substrate faced the photoactive area of one PV module each.

2.6. Structural and Thermal Characterization. ^{1}H-NMR (400 MHz) spectra were recorded on a Bruker Avance 400 using deuterated DMSO as the solvent. FTIR spectra were recorded using a Thermo Nicolet Nexus 670 instrument. Measurements were performed on solids coated on KBr discs, recording 64 accumulated scans at a resolution of 2 cm^{-1}. GPC analyses were performed on an apparatus consisting of a Waters 515 HPLC pump (mobile phase, THF; flow rate, 1 mL/min, at 35 °C), three Styragel columns (models HR 4, HR 3, and HR 2) from Waters, and a refractive index detector Waters 2410. Samples were dissolved in THF at concentrations of 0.2 wt %. A calibration curve was prepared using monodispersed fractions of polystyrene. Differential scanning calorimetry (DSC) analyses were performed with a DSC 823e Mettler-Toledo instrument by applying the following thermal cycle: from 25 to 180 °C, from 180 to −50 °C, and from −50 to 180 °C. The heating/cooling rate was 20 °C/min. Thermogravimetric analyses (TGA) were performed with a Q500 TGA system (TA Instruments) from rt to 800 °C at a scan rate of 10 °C/min in an air atmosphere.

2.7. Optical Characterization. UV−visible spectroscopy analyses were performed at rt on a Thermo Scientific Evolution 600 UV−vis spectrophotometer. Relative reflectance was measured on a Jasco V-570 UV−vis−NIR spectrophotometer equipped with an integrating sphere and a PTFE foil as reference. Refractive index was measured using a Filmetrics F20 thin-film analyzer in the wavelength range of 400−800 nm and the BK7 reflection standard was used to calibrate the instrument in the contact stage mode. The samples for refractive index analysis were prepared by spin-coating (600 rpm, 60 s) a chloroform solution of PU-Cou (80 mg/mL) on a silicon wafer substrate, followed by UVA irradiation for cross-linking. Fluorescence spectra were recorded on a Jasco FP-6600 spectrofluorometer. Photoluminescence quantum yield of cross-linked PU-Cou was measured on a FluoroMax-2 spectrofluorometer equipped with an R928 photomultiplier tube. Optical and fluorescence micrographs were recorded through a Leica DMI3000B fluorescence microscope equipped with a digital camera, using specific filters depending on the excitation and emission wavelengths of the investigated samples. Device efficiency measurements were performed using an Abet Technologies Sun 2000 solar simulator with AM1.5G filter. A Keithley 2612B source-measuring unit was used to perform the voltage scans and measure the current output. The data obtained were averaged out of at least three different devices.

2.8. Photochemical Stability and Surface Properties. Weathering tests were performed in a Solarbox 3000e weather-o-meter chamber (Cofomegra srl), equipped with a xenon lamp and an outdoor filter ($\lambda > 280$ nm). The total applied irradiance was equal to 550 W/m^2 in the 300−800 nm range at a temperature of 40 °C and an average relative humidity of 25%. Adhesion strength of the coatings on glass substrates was determined through a PosiTest AT-M Manual pull-off tester (DeFelsko) by measuring the pulling force needed to detach a 20 mm diameter aluminum dolly glued to the cross-linked coatings by means of a two-component epoxy adhesive (Araldite 2011, curing cycle: 50 °C, 24 h). Wettability was studied in terms of static optical contact angle (OCA) measurements, which were performed with OCA 20 (DataPhysics) equipped with a CCD photocamera and with a 500 μL Hamilton syringe to dispense liquid droplets. Water and diiodomethane (CH_2I_2) were used as probe liquids. The surface energy of the coatings was calculated according to the Owens−Wendt−Rabel−Kaelble (OWRK) method.[48]

3. RESULTS AND DISCUSSION

3.1. Synthesis and Characterization of Coumarin-Functionalized Polyurethane (PU-Cou). The photoresponsive polyurethane was obtained by a one-step reaction between a commercial aliphatic isocyanate prepolymer (Desmodur XP 2599, from here on referred to as DX2599) and a coumarin derivative (7-(hydroxy ethoxy)-4-methylcoumarin, HEOMC) (Scheme 1A). Since aliphatic alcohols exhibit higher reactivity toward isocyanate addition compared to the aromatic ones,[49] 7-hydroxy-4-methylcoumarin (HMC) was reacted with 2-bromoethanol to obtain an aliphatic alcohol (HEOMC).[36] Indeed, the reaction was complete in 2 h at rt and the coumarin-modified prepolymer (PU-Cou) was obtained in excellent yield. The modification was studied by FTIR spectra (Figures 1A and S1 in the Supporting Information). Specifically, the signals at 3440 cm^{-1} (O−H stretching) and 2270 cm^{-1} (N=C=O stretching) associated with HEOMC and isocyanate precursor, respectively, are absent in the final product, confirming full conversion of isocyanate and alcohol groups. Moreover, the peaks appearing in the PU-Cou spectrum at 3075 cm^{-1} (unsaturated C−H stretching), 1618 cm^{-1} (C=C stretching in pyrone rings), and 1152 cm^{-1} (C−H bending in pyrone rings)[50] confirmed the incorporation of coumarin moieties in the prepolymer. GPC analyses evidenced a clear increase in the number average

Scheme 1. (A) Functionalization of Polyisocyanate (DX2599) with Coumarin Precursor (HEOMC) and (B) Reversible Cross-Linking of PU-Cou via Photoinduced [2+2] Dimerization of Coumarin Groups

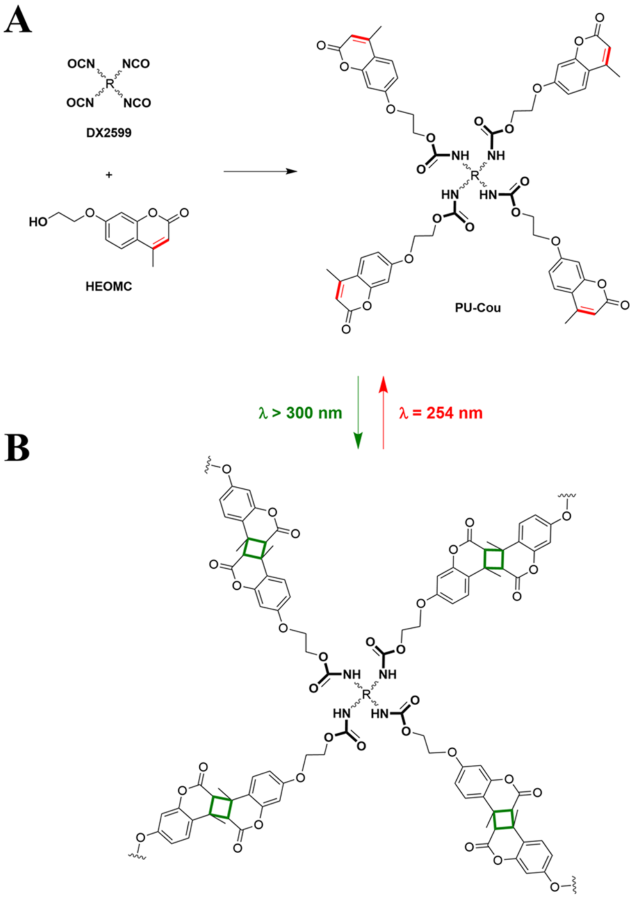

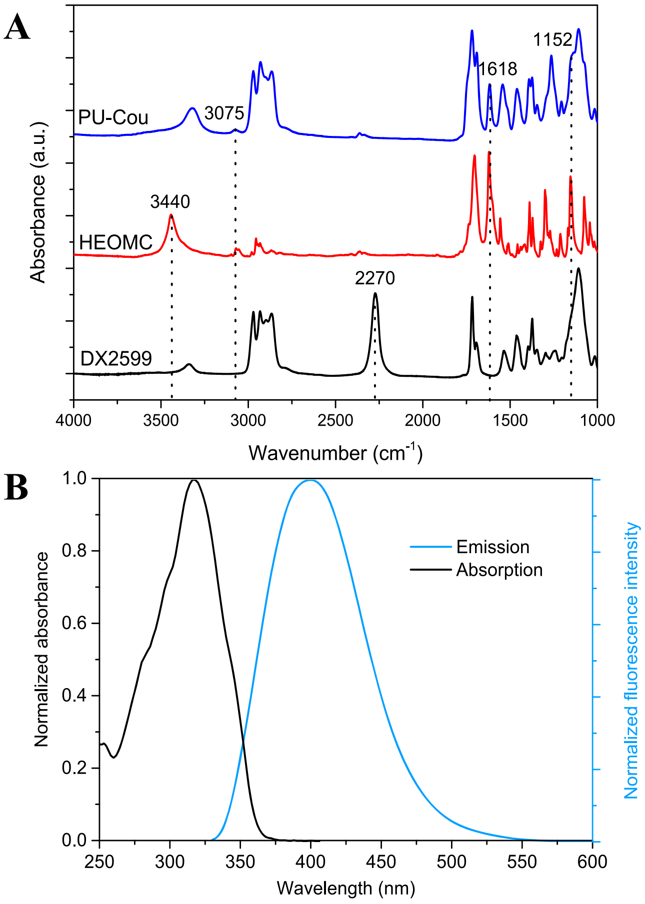

Figure 1. (A) FTIR spectra of isocyanate prepolymer (DX2599), 7-(hydroxy ethoxy)-4-methylcoumarin (HEOMC) precursors, and coumarin-modified prepolymer (PU-Cou). (B) Normalized UV−vis absorption and fluorescence emission spectra of PU-Cou.

molecular weight (M_n) from 3210 g/mol for the isocyanate prepolymer to 4370 g/mol for PU-Cou, while polydispersity index ($Đ$) was around 1.1 for both the macromers, providing further confirmation of functionalization.

UV−vis absorption spectrum (Figure 1B) of PU-Cou coated on quartz displayed a broad, intense signal around 320 nm, which is characteristic of substituted coumarins and related to overlapping $\pi-\pi^*$ electron transitions of conjugated benzene and pyrone chromophores.[51] Moreover, the fluorescence emission spectrum, with 320 nm as the excitation wavelength, exhibited a broad band peaking at λ = 394 nm (blue curve), which is typical of coumarin derivatives bearing electron-donating groups at position 7, as the precursor HEOMC.[52]

3.2. Photoinduced Cross-Linking and Characterization.

The photoreactivity of PU-Cou was studied by recording UV−vis spectra of thin films spin-coated on quartz slides after different time intervals of exposure under the UVA source (λ > 300 nm). As evidenced in Figure 2A, the strong absorption signal at around 320 nm gradually decreased with the irradiation time. As the double bonds of coumarin groups reacted to form the cyclobutane rings by [2+2] cycloaddition (Scheme 1B), the conjugation is progressively lost, leading to a decrease in the absorbance.[29,31] The extent of the conversion of pendant coumarin groups into photodimers (dimerization degree, DD%) was calculated according to the following equation[36]

$$\mathrm{DD}\ \% = \left(1 - \frac{A_t}{A_0}\right) \times 100 \tag{1}$$

where A_0 and A_t are the absorption intensities at 320 nm before and after a time t of UV exposure, respectively. As shown in Figure 2B, the dimerization degree increases over time and reaches a plateau after 120 min of exposure, corresponding to conversion of 93.2%, in line with previously reported systems.[37,53] As reported in Figure 2C, the UVA treatment for 120 min (corresponding to the maximum conversion of coumarin groups) strongly reduced the fluorescence intensity at 394 nm, owing to the decrease in the concentration of luminophores in dimerized PU-Cou.[54] Nevertheless, the decrease was only 68.8%, significantly lower than the one calculated from the absorbance spectra (93.2%). The difference can be explained by considering that a lower number of coumarin chromophores also results in a lower probability of reabsorption/re-emission events, as suggested by the slight blue shift in the fluorescence spectrum of dimerized PU-Cou with respect to as-cast material.

Owing to the high functionality of PU-Cou (around 4.2 coumarin units per mole, based on the NCO/mole ratio of the parent polyisocyanate), the UVA photoinduced dimerization process of coumarin moieties is expected to yield photocuring of the material. Indeed, upon UVA irradiation, the soluble macromer turned into an insoluble, densely cross-linked network, as evidenced by gel content measurements. Specifically, PU-Cou was spin-coated from chloroform solutions on glass slides and irradiated under UVA (120 min). The obtained samples, with an average thickness of 1.5 μm, were immersed in chloroform for 24 h and the residual insoluble content was found to be >95%, consistent with the dimerization degree calculated by UV−vis spectroscopy.

An extensive characterization of cross-linked PU-Cou was performed in terms of thermal, optical, and surface properties to assess its relevance for optical coating applications. As for thermal characterization, DSC traces evidenced a single glass transition (T_g) at around 50 °C for the cross-linked polymer (see Figure S2 in the Supporting Information), while the pristine PU-Cou macromer displayed a broad melting transition around 70 °C, which was evidently suppressed after the UV-induced dimerization. The decomposition profile, measured by TGA in air, did not show any degradation event before 210 °C (Figure S3 in the Supporting Information), thus demonstrating the excellent thermal stability of the cross-linked material.[55] As for the optical properties, coatings were visually clear and colorless after the UVA irradiation, with a transmittance greater than 90% in the 400−900 nm range (Figure 2D). Specifically, no discoloring was observed, owing to the inherent UV stability of aliphatic polyurethanes compared to the aromatic ones.[56] Such high transparency was retained even during a long-term (>500 h) accelerated weathering test under continuous white-light illumination (Figure S4, Supporting Information), clearly evidencing the excellent photostability of the cross-linked PU-Cou system and confirming its potential suitability for outdoor use. Furthermore, the reflectance was as low as 8.0% over the 400−800 nm spectral range and the refractive index resulted to be 1.51 (λ = 589 nm). Both values were close to those reported for commercial PMMA and, combined with its high transparency, demonstrated the suitability of cross-linked PU-Cou as a potential host matrix for LSCs.[11] The LQY of the cross-linked coatings resulted to be 26.7%. Regarding surface properties,

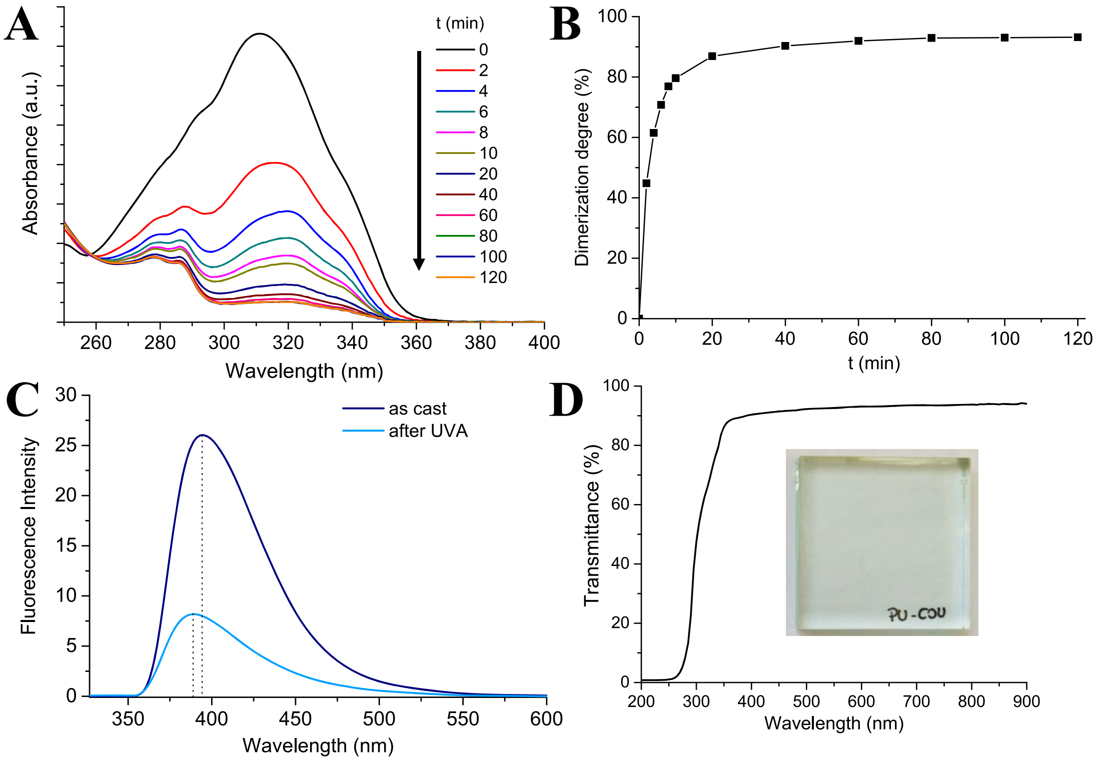

Figure 2. (A) UV−vis absorption spectra of PU-Cou coating and (B) percent conversion of coumarin groups into dimers as a function of different UVA ($\lambda > 300$ nm) irradiation times. (C) Fluorescence emission spectra of pristine PU-Cou and after UVA irradiation ($\lambda > 300$ nm, 120 min). (D) UV−vis transmission spectrum of PU-Cou after irradiation ($\lambda > 300$ nm, 120 min); inset: picture of the cross-linked PU-Cou coated on a glass slab, evidencing its excellent transparency in the visible spectrum.

static contact angle measurements evidenced moderate hydrophobicity ($\vartheta_{H_2O} = 93°$) and surface energy ($\gamma = 46.12$ mN/m) predominantly determined by the dispersive component ($\gamma_d = 46.01$ mN/m). Lastly, the adhesion strength on glass obtained from pull-off tests was found to be higher than 16 MPa, with cohesive failure in the glass substrate and no detachment of the coating. The value is particularly remarkable in view of the application of this material as a functional coating for transparent substrates, e.g., on retrofitted windows.

3.3. Photoinduced Network Reversibility and Self-Healing. The cross-linked coatings were irradiated under monochromatic UVC light ($\lambda = 254$ nm). As evidenced by the progressive increase of the absorption signal at around 320 nm (Figure 3A), the photocleavage of cyclobutane adducts in the dimers restores the conjugation of the coumarin moieties (Scheme 1B). The DD% decreased over time reaching a plateau at 23% (Figure 3B), implying that the photocleavage was not complete. This feature is generally observed in coumarin-based photoreversible polymer networks when irradiated in the solid state and it is ascribed to a dynamic equilibrium between cycloaddition and its reverse.[30,31,39] Fluorescence emission spectra (Figure 3C) evidenced the high degree of recovery (≈85%) of the original emission intensity after UVC irradiation. FTIR analysis, performed on thin films coated on KBr crystal windows, allowed to monitor structural changes after the UVA/UVC irradiation cycles. In accordance with the literature,[36] the spectrum of pristine, un-cross-linked PU-Cou presented two relevant signals in the 1800−1600 cm^{-1} spectral range: the band centered at 1718 cm^{-1} (C═O of pyrone ring overlapped with C═O in polyurethane) and the one at 1618 cm^{-1} (C═C of pyrone ring overlapped with phenyl ring). Upon UVA irradiation, a shoulder peak appeared at 1760 cm^{-1}, while the band at 1618 cm^{-1} decreased and shifted, indicating conversion of double bonds. The subsequent UVC irradiation allowed to restore the structural changes (Figures 3D and S5 in the Supporting Information).

Photoinduced dimerization and cleavage were performed cyclically by alternating UVA and UVC irradiations (Figure 4A). The slight decrease in the efficiency of the dimerization/cleavage process upon repeated cycles is commonly observed in coumarin-based systems and attributed to side reactions during the 254 nm treatment, which cause the formation of nonreversible adducts and/or cleavage byproducts.[30,39] Nevertheless, the polymer network displayed high reversibility and recovery of fluorescence during multiple cycles (Figure 4B). Indeed, full reversibility on a molecular scale is not a necessary condition for complete aesthetical and functional recovery of the coating surface, as confirmed by qualitative self-healing tests. The PU-Cou coating was cross-linked under UVA and its surface was damaged by means of a scalpel, producing scratches with an average width of 30−40 μm and depth lower than the coating thickness (Figure 4C). Upon exposure to UVC ($\lambda = 254$ nm, 160 min) followed by UVA ($\lambda > 300$ nm, 120 min), complete repair was observed (Figure 4D). Exposure times were established to maximize the number of free coumarins generated during the photocleavage and the number of dimer adducts during the photo-cross-linking stage, on the basis of the kinetics determined by UV−vis spectroscopy. Two control experiments were performed to elucidate the specific role of [2+2] photocycloaddition in the repairability of the polymer matrix. First, when the damaged samples were directly irradiated for 5 h under UVA only, no

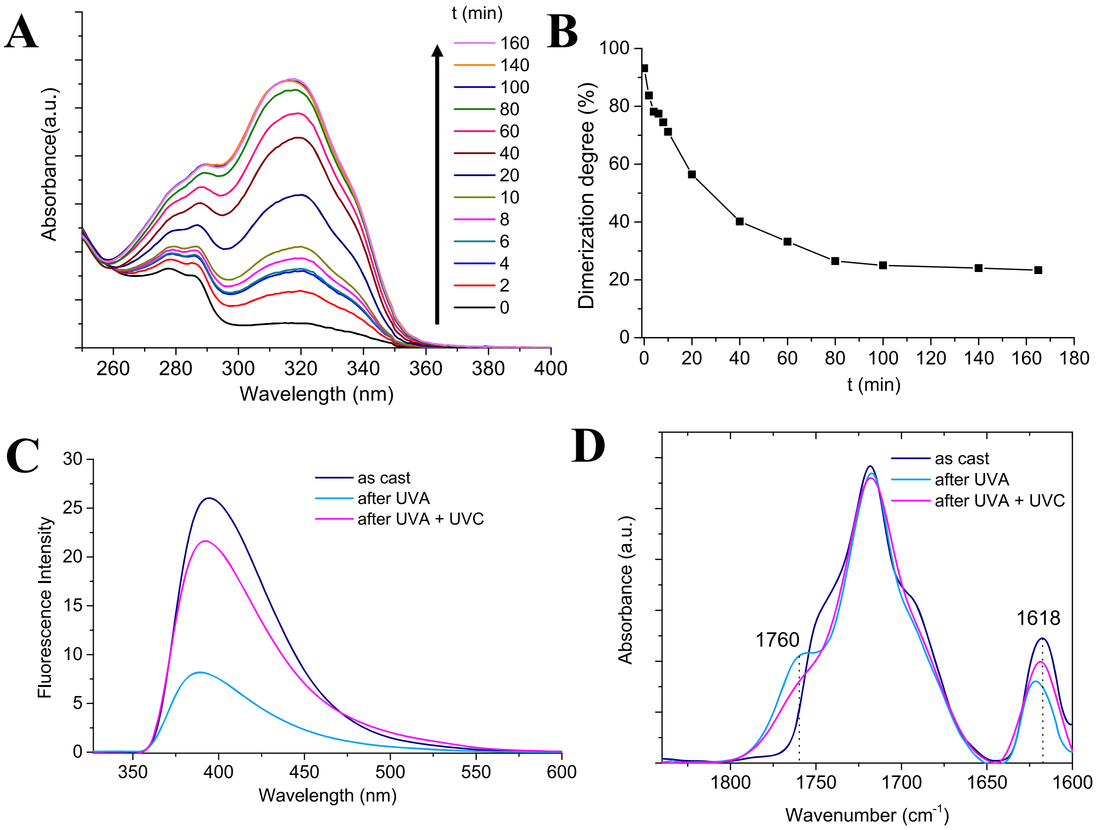

Figure 3. (A) UV−vis absorption spectra of PU-Cou coating and (B) percent conversion of coumarin groups into dimers as a function of different UVC (λ = 254 nm) irradiation times. (C) Fluorescence emission spectra and (D) details of FTIR spectra of pristine PU-Cou, after UVA irradiation (λ > 300 nm, 120 min), and after one UVA-UVC (λ = 254 nm, 160 min) cycle (signals normalized with respect to the band centered at 1718 cm^{-1}).

healing was observed (Figure S6A, Supporting Information). This indicates that the sole mechanical damage, which is commonly considered to occur preferentially at the cyclobutane cross-links, does not generate enough free coumarin moieties able to promote healing through UVA re-cross-linking. As a consequence, a preliminary UVC treatment for photocleavage is necessary to achieve the repair, in accordance with the majority of previously reported systems.[29,36,38] Second, when damaged samples were heated at 60 °C (i.e., above the T_g) for 5 h in the dark, no healing was observed, pointing out that the sole thermal stimulus was not able to induce repair (Figure S6B, Supporting Information). The photoinduced healing ability in the presence of multiple surface scratches was also investigated. As more extensively discussed in Section S6 in the Supporting Information, optical microscopy and profilometric analyses proved the full repair of the PU-Cou coating after healing treatment (UVC+UVA). These results further demonstrate the excellent photoinduced healing ability of our system.

3.4. Dye Incorporation and Optical Characterization.

Given the excellent thermal, optical, and functional characteristics of this photoresponsive coumarin-based coating system, its suitability as host matrix material for LSC application was investigated by doping PU-Cou with two distinct fluorophores: Lumogen F Red 305 (LR305) and Coumarin 6 (C6), selected because of their wide availability, high LQY (>95%), and broad Stokes shift.[12] In particular, LR305 represents the state-of-the-art in organic dopants for LSCs,[2,57,58] while C6, a widely used fluorescent dye,[59] only recently was proposed as a luminescent dopant for this application.[60] Each dye was combined with PU-Cou in chloroform solution, spin-coated on glass slabs, and irradiated under UVA for 120 min to ensure maximum cross-linking of the polymer matrix. The obtained coatings were visually clear and homogeneous. Upon immersing the coated slides in chloroform for 24 h under stirring, the dyes were completely extracted from the cross-linked PU-Cou coatings, as confirmed by UV−vis spectroscopy (Figure S9, Supporting Information). Thus, no chemical interaction between the embedded fluorescent dyes and the host matrix was found to occur during the UVA treatment to induce cross-linking.

To gain preliminary insights into the optical properties of the selected fluorophores, a first characterization by means of UV−vis and fluorescence spectroscopy was performed on LR305 and C6 dispersed in a reference polymeric matrix (i.e., PMMA) subjected to the same UVA treatment used on PU-Cou coatings. The absorption spectrum of LR305/PMMA (Figure 5A) exhibited the two characteristic peaks of LR305 (445 and 575 nm) and a peak at 611 nm in the fluorescence emission spectrum, in accordance with the literature.[21,61] As for C6/PMMA, the peak at 444−450 nm in the absorption spectrum and the one at 539 nm in the emission profile (Figure 5B) are indicative of coumarin derivatives substituted with an amino group at the 7 position of the benzene ring, as in C6.[52,62,63] In addition, the spectral overlap of the absorption spectrum of the luminophore (acceptor species) with the emission spectrum of the undoped cross-linked PU-Cou coating (donor specie) suggested possible occurrence of energy transfer via fluorescence resonance mechanism

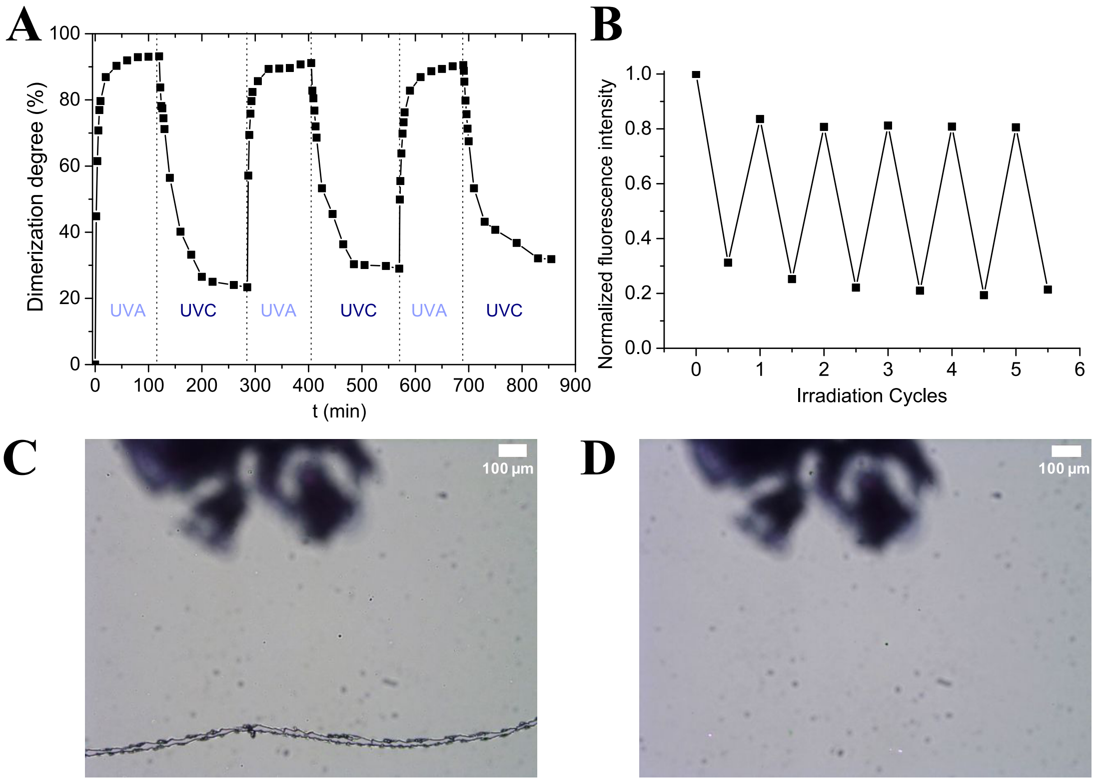

Figure 4. (A) Dimerization degree upon alternating exposure under UVA (λ > 300 nm, 120 min) and UVC (λ = 254 nm, 160 min) calculated from absorption intensity at 320 nm. (B) Fluorescence emission at 394 nm upon subsequent irradiation cycles (UVA+UVC). (C) Cross-linked PU-Cou coating damaged with a scalpel. (D) PU-Cou fully repaired after healing treatment (UVC+UVA) at rt.

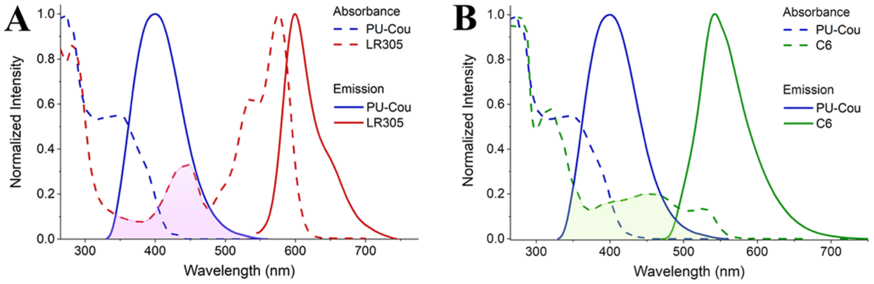

Figure 5. Normalized absorption and emission spectra (λ_{exc} = 327 nm) of the undoped cross-linked PU-Cou (donor) compared to the luminophore acceptors (A) LR305 and (B) C6 dispersed in PMMA. The colored areas indicate the overlap between the emission of the donor and the absorption of the acceptor.

(FRET) from the host matrix to the luminescent species.[64−68] Indeed, the values of spectral overlap integral (see the Supporting Information for details on the calculation) resulted to be 2.93×10^{-14} and 7.42×10^{-15} cm^3 M^{-1} for LR305- and C6-doped PU-Cou, respectively, in line with those reported in the literature.[69] A deeper analysis of the FRET mechanism is presented in the Supporting Information (Section S8).

UV−vis absorption spectra performed on LR305/PU-Cou highlighted the contribution of the absorption features of both the matrix and the dye (Figure 6A). Owing to the complete transparency of the cross-linked PU-Cou in the visible range, the characteristic peaks of the perylene-based dye could be clearly observed. Furthermore, by increasing the concentration of the dye from 1 to 7 wt %, the absorbance (λ_{max} = 577 nm) linearly increased, while a progressively decreased solubility of LR305 in PU-Cou at higher concentrations caused deviation from linearity.

Fluorescence emission spectra (λ_{exc} = 327 nm, recorded in front-face configuration) evidenced a strong emission signal peaking at 611 nm, contributed by both the matrix and the dye through energy transfer, as previously discussed. The intensity of the fluorescence peak was found to increase gradually with the absorbance up to $A \approx 0.45$ (corresponding to 5 wt % LR305), while, above this threshold, a gradual decrease was observed (Figure 6B). Furthermore, a bathochromic shift of the emission peak was observed in normalized emission spectra (Figure 6C), typical of highly doped LSCs and ascribed to a higher probability of reabsorption processes and to aggregation of dye molecules.[39,70−72]

In contrast to what was observed in LR305/PU-Cou systems, a markedly different optical behavior was reported for C6/PU-Cou, resulting in maximum optical performance for 3 wt % C6 doping level (see Section S12 in the Supporting Information).

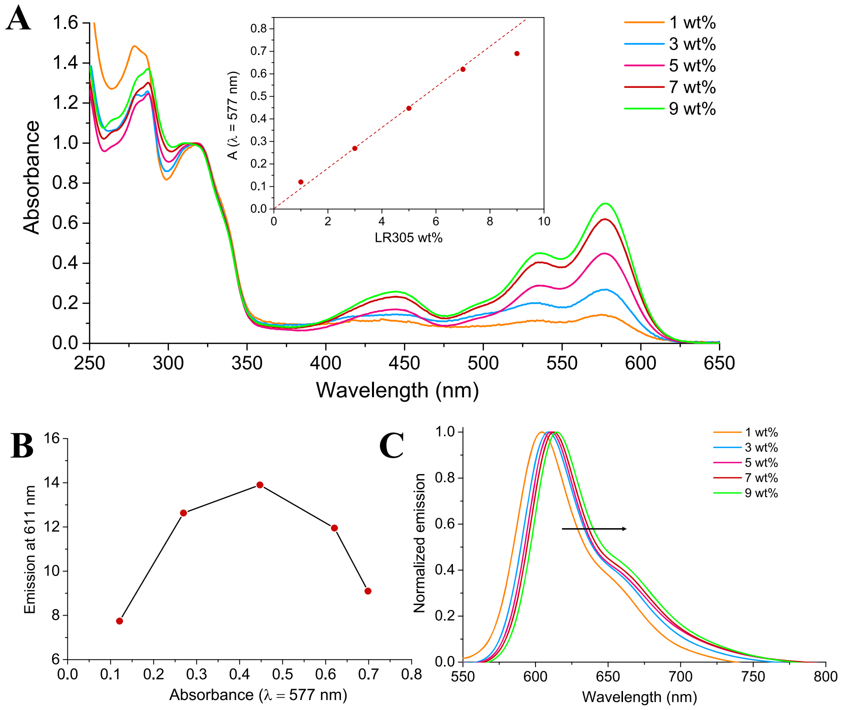

Figure 6. Optical properties of cross-linked PU-Cou doped with LR305. (A) UV−vis absorption spectra at increasing luminophore concentrations; inset: absorbance at 577 nm vs luminophore concentration (dashed line shows linear fit of the experimental data; fitting equation: $y = 0.09x$, with $R^2 = 0.99$). (B) Emission intensity at ≈611 nm peak vs absorbance at 577 nm. (C) Normalized fluorescence emission spectra at increasing luminophore concentration ($\lambda_{exc} = 327$ nm).

3.5. LSC Device Characterization and Photoinduced Healing. Considering the favorable optical characteristics of luminophore-doped PU-Cou self-healing coatings (5 wt % LR305 or 3 wt % C6), their performance as thin-film LSCs was evaluated in the presence of edge-coupled c-Si PV cells (see the Experimental Section for details) by calculating the so-called device efficiency (η_{LSC})[60]

$$\eta_{LSC} = \frac{FF \cdot I_{SC} \cdot V_{OC}}{P_{IN} \cdot A_{LSC}} \tag{2}$$

where A_{LSC} is the active (top) area of the LSC device; P_{IN} is the incident solar-simulated power density; and FF, I_{SC}, and V_{OC} are the fill factor, the short-circuit current, and the open-circuit voltage of the edge-coupled PV cells, respectively. To ensure reliability in the measurements, a dark absorbing background was used underneath the LSC slab and no reflective elements were placed at the free edges of the light guide. In this way, reflections and backscattered light from inside or outside the waveguide as well as multiple-pass of photons could be excluded, thus avoiding overestimation of the obtained results. In addition, direct illumination of the edge-mounted PVs was carefully prevented. In these experimental conditions, overall (four edges) η_{LSC} values as high as 1.16 ± 0.06% for LR305/PU-Cou and 0.64 ± 0.04% for C6/PU-Cou could be achieved, which are in line with recently reported results on other thin-film LSCs using similar fluorophores as luminescent species and tested in analogous conditions.[73,74] To assess the contribution of our UV-responsive, self-healing matrix to the obtained PV performance, convenient benchmark LSC devices were obtained by coating glass slabs with doped PMMA, the latter being selected as the reference host matrix given its wide use in the field. The concentration of LR305 and C6 in PMMA was adjusted in such a way as to obtain LSCs with the same optical density (OD, evaluated at λ_{max}) as those based on our PU-Cou matrix, namely, OD ≈ 0.61 for LR305 and OD ≈ 0.18 for C6. Under the same experimental conditions previously described, the η_{LSC} values of such PV-coupled LSCs were 1.20% for LR305/PMMA and 0.66% for C6/PMMA, thus comparable with the ones obtained with our photoresponsive systems. This result further confirms the factual potential of PU-Cou as a host matrix material for high-efficiency LSCs.

Then, to evaluate the effect of surface damages on the performance of PV-coupled LSCs and to demonstrate the photoinduced healing ability of the new PU-Cou LSC system, tests were performed on scratched LSC coatings prior to and after UV healing treatment. As shown in Figure 7, by damaging the surface of the LSC with a scalpel to induce a single 20−30 μm wide scratch, a non-negligible reduction of device performance could be observed compared with the pristine undamaged LSCs (namely, a ∼5 and ∼7% loss in η_{LSC} for LR305-doped and C6-doped matrix, respectively). Indeed, an increase in surface roughness resulting from the mechanical damage determines a higher probability of light-scattering events at defects generated on the coating surface, leading to a reduced ability to trap traveling photons within the host matrix. Upon UV-induced healing, namely, by irradiating the damaged samples at 254 nm (160 min), followed by UVA ($\lambda >$ 300 nm) treatment for 120 min, complete disappearance of the surface scratches was reported from optical micrographs on both LR305- and C6-doped LSC systems, paired with complete recovery (∼100%) of the original LSC performance (Figure 7C,E). These results clearly demonstrate the excellent photoinduced healing capabilities of these systems also in the presence of a luminescent dopant and provide evidence of their potential in restoring esthetic and functional properties in

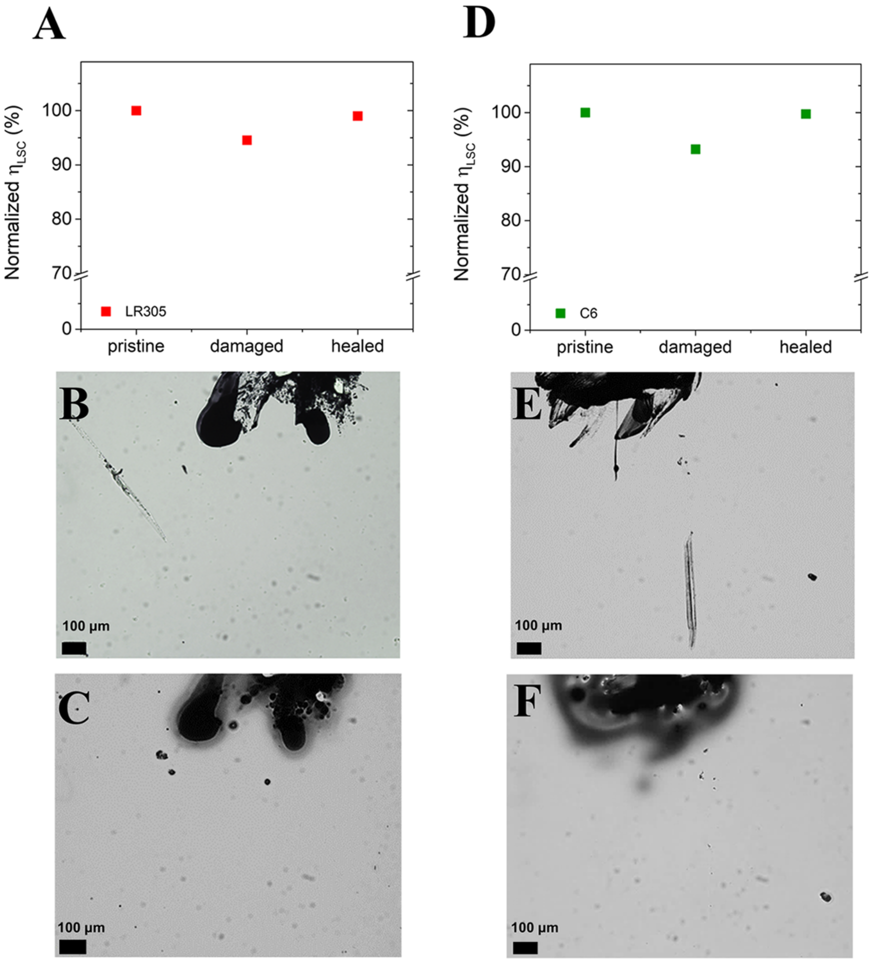

Figure 7. (A, D) Normalized device efficiency values of photoreversible PU-Cou matrix doped with 5 wt % LR305 or 3 wt % C6, respectively, before the damage, damaged, and after UV-induced healing. An appreciable reduction of device performance was detected after damaging the surface of the LSC with a single scratch. The excellent healing capabilities of these systems become crucial when a more significant device performance drop is expected as a result of multiple surface scratches. Optical microscope images of LR305/PU-Cou (B) damaged and (C) UV-repaired and of C6/PU-Cou (E) damaged and (F) UV-repaired.

operating LSCs in an easy and straightforward manner. In particular, the self-healing response of these systems may become crucial in the presence of multiple surface scratches, which would be expected to yield a significant device performance drop. To investigate this aspect, LSCs with an increasing number of surface damages were prepared and their performance after both scratching and light-induced healing cycles were recorded as a function of the damage level. These experiments were carried out only on LR305/PU-Cou LSC devices, as it was previously demonstrated that the addition of the luminophore into the PU-Cou matrix does not affect the photoinduced healing response of the coating. As illustrated in Figure 8A, the presence of a higher number of surface cuts led to a sharper drop in η_{LSC} compared with the single-scratch system (namely, a ~5 and ~11% loss in η_{LSC} for single-scratch and multiple-scratch LSC samples, respectively), ascribable to a progressively lower ability to trap traveling photons within the waveguide. Interestingly, after irradiation treatment, the multiple surface scratches were completely repaired and the η_{LSC} of the correspondingly healed LSC devices resulted to be comparable to that obtained for pristine samples. This effect could be attributed to the ability of the [2+2] photoreversible cycloaddition reaction occurring at a molecular level to re-establish the original surface smoothness of the coating, as demonstrated by the results of profilometric analysis (Figures S7 and S8, Supporting Information).

Finally, the performance of large-area LSC samples damaged with multiple scratches and healed via the proposed light-exposure treatment was evaluated to elucidate the role of mechanically induced surface scattering on the overall device efficiency for increasing LSC dimensions. More specifically, 5 × 5 cm^2, 10 × 10 cm^2, and 15 × 15 cm^2 LR305/PU-Cou LSCs were produced and the value of η_{LSC} in pristine, damaged, and healed LSC devices with different dimensions was recorded. To ensure reproducibility, the same scratch pattern was used on all LSCs to obtain the same level of surface damage, as schematically depicted in Figure 8B. Interestingly, a clear reduction in η_{LSC} values was observed for scratched LSCs of increasing dimension. This confirms the detrimental effect of the presence of imperfections and optical defects at the waveguide/air interface on LSC performance even in the case of larger-area LSC devices, thus further highlighting the relevance of the photoresponsive polymer matrix presented in this work also in real larger-scale applications.

4. CONCLUSIONS

A coumarin-based, photoresponsive polymer coating exhibiting excellent UV-induced self-healing capabilities was demonstra-

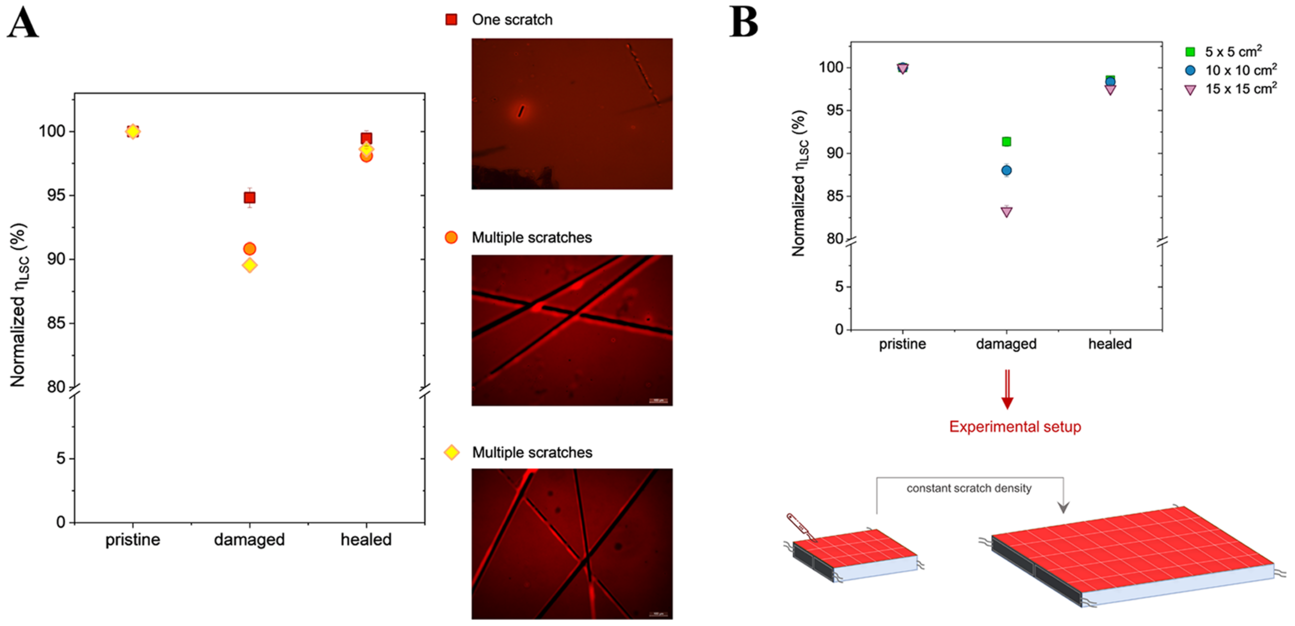

Figure 8. (A) Normalized device efficiency values of PU-Cou matrix doped with 5 wt % LR305 before the damage (pristine), damaged, and after UV-induced healing (healed) as a function of the damage level. An increasing reduction of device performance was recorded after damaging the surface of the LSC with a larger number of scratches. Fluorescence microscopy images of corresponding damaged LR305/PU-Cou systems are also reported. (B) Normalized device efficiency values of PU-Cou matrix doped with 5 wt % LR305 before the damage (pristine), damaged, and after UV-induced repair (healed) considering increasingly larger-area LSCs (5 × 5 cm^2, 10 × 10 cm^2, and 15 × 15 cm^2). As depicted schematically at the bottom, the scratching pattern applied onto 5 × 5 cm^2 LSCs was repeated onto larger-area LSC devices to maintain a fixed damage density on LSC with increasing area.

ted in this work for application as a host matrix in thin-film LSC devices. This cross-linked polymeric system is characterized by high optical transmittance (>90%) in the visible spectrum and by remarkable molecular reversibility, which results in outstanding light-induced self-healing behavior. Indeed, healing of surface scratches could be possible solely by UV irradiation, with no need for additional thermal treatment.

LSC devices based on such photoresponsive coatings incorporating suitable luminescent species yielded PV performance comparable with reference thin-film LSCs based on state-of-the-art matrixes (i.e., PMMA), thus ranking this functional LSC platform among the best-performing systems in the field, with the valuable advantage of providing additional light-induced healing ability. In particular, the decline in PV performance experienced by mechanically scratched LSCs could be fully recovered upon a suitable UV irradiation cycle, as a result of the successful healing process provided by the reversible [2+2] cleavage/dimerization photocycloaddition of the coumarin-based moiety.

This work provides the first demonstration of optically transparent, photoreversible polymeric host matrixes for LSCs with high efficiency and excellent healing capabilities, thus enabling the development of stimuli-responsive durable LSC devices with added functionalities.

■ ASSOCIATED CONTENT

Supporting Information

The Supporting Information is available free of charge at https://pubs.acs.org/doi/10.1021/acsapm.0c00515.

> PU-Cou synthesis monitored by FTIR; DSC of pristine and cross-linked PU-Cou; TGA of cross-linked PU-Cou; weathering test of undoped cross-linked PU-Cou; photoinduced reversibility of the polymer network monitored by FTIR; self-healing; extraction in solvent; fluorescence resonance energy transfer (FRET); C6/PU-Cou as-cast/cross-linked coatings at different luminophore concentrations; effect of repeated UV irradiation (PDF)

■ AUTHOR INFORMATION

Corresponding Author

Gianmarco Griffini − *Department of Chemistry, Materials and Chemical Engineering "Giulio Natta", Politecnico di Milano, 20133 Milano, Italy;* orcid.org/0000-0002-9924-1722; Email: gianmarco.griffini@polimi.it

Authors

Giovanni Fortunato − *Department of Chemistry, Materials and Chemical Engineering "Giulio Natta", Politecnico di Milano, 20133 Milano, Italy;* orcid.org/0000-0002-8922-8081

Elisavet Tatsi − *Department of Chemistry, Materials and Chemical Engineering "Giulio Natta", Politecnico di Milano, 20133 Milano, Italy*

Francesca Corsini − *Department of Chemistry, Materials and Chemical Engineering "Giulio Natta", Politecnico di Milano, 20133 Milano, Italy*

Stefano Turri − *Department of Chemistry, Materials and Chemical Engineering "Giulio Natta", Politecnico di Milano, 20133 Milano, Italy;* orcid.org/0000-0001-8996-0603

Complete contact information is available at: https://pubs.acs.org/10.1021/acsapm.0c00515

Notes

The authors declare no competing financial interest.

■ ACKNOWLEDGMENTS

Authors greatly acknowledge Gigliola Clerici for her kind support with DSC analysis.

■ REFERENCES

(1) Biyik, E.; Araz, M.; Hepbasli, A.; Shahrestani, M.; Yao, R.; Shao, L.; Essah, E.; Oliveira, A. C.; del Caño, T.; Rico, E.; Lechón, J. L.; Andrade, L.; Mendes, A.; Atlı, Y. B. A Key Review of Building Integrated Photovoltaic (BIPV) Systems. *Eng. Sci. Technol. Int. J.* **2017**, *20*, 833−858.

(2) Debije, M. G.; Verbunt, P. P. C. Thirty Years of Luminescent Solar Concentrator Research: Solar Energy for the Built Environment. *Adv. Energy Mater.* **2012**, *2*, 12−35.

(3) Meinardi, F.; Bruni, F.; Brovelli, S. Luminescent Solar Concentrators for Building-Integrated Photovoltaics. *Nat. Rev. Mater.* **2017**, *2*, 1−9.

(4) Traverse, C. J.; Pandey, R.; Barr, M. C.; Lunt, R. R. Emergence of Highly Transparent Photovoltaics for Distributed Applications. *Nat. Energy* **2017**, *2*, 849−860.

(5) Griffini, G. Host Matrix Materials for Luminescent Solar Concentrators: Recent Achievements and Forthcoming Challenges. *Front. Mater.* **2019**, *6*, 1−8.

(6) McKenna, B.; Evans, R. C. Towards Efficient Spectral Converters through Materials Design for Luminescent Solar Devices. *Adv. Mater.* **2017**, *29*, No. 1606491.

(7) Pucci, A. Luminescent Solar Concentrators Based on Aggregation Induced Emission. *Isr. J. Chem.* **2018**, *58*, 837−844.

(8) Moraitis, P.; Schropp, R. E. I.; Van Sark, W. G. J. H. Nanoparticles for Luminescent Solar Concentrators - A Review. *Opt. Mater.* **2018**, *84*, 636−645.

(9) Zhou, Y.; Zhao, H.; Ma, D.; Rosei, F. Harnessing the Properties of Colloidal Quantum Dots in Luminescent Solar Concentrators. *Chem. Soc. Rev.* **2018**, *47*, 5866−5890.

(10) Griffini, G.; Brambilla, L.; Levi, M.; Castiglioni, C.; Del Zoppo, M.; Turri, S. Anthracene/Tetracene Cocrystals as Novel Fluorophores in Thin-Film Luminescent Solar Concentrators. *RSC Adv.* **2014**, *4*, 9893−9897.

(11) Zettl, M.; Mayer, O.; Klampaftis, E.; Richards, B. S. Investigation of Host Polymers for Luminescent Solar Concentrators. *Energy Technol.* **2017**, *5*, 1037−1044.

(12) Tummeltshammer, C.; Taylor, A.; Kenyon, A. J.; Papakonstantinou, I. Losses in Luminescent Solar Concentrators Unveiled. *Sol. Energy Mater. Sol. Cells* **2016**, *144*, 40−47.

(13) Thomas, W. R. L.; Drake, J. M.; Lesiecki, M. L. Light Transport in Planar Luminescent Solar Concentrators: The Role of Matrix Losses. *Appl. Opt.* **1983**, *22*, 3440.

(14) Zhang, F.; Ju, P.; Pan, M.; Zhang, D.; Huang, Y.; Li, G.; Li, X. Self-Healing Mechanisms in Smart Protective Coatings: A Review. *Corros. Sci.* **2018**, *144*, 74−88.

(15) Delgado-Sanchez, J. M. Luminescent Solar Concentrators: Photo-Stability Analysis and Long-Term Perspectives. *Sol. Energy Mater. Sol. Cells* **2019**, *202*, No. 110134.

(16) Liu, G.; Mazzaro, R.; Wang, Y.; Zhao, H.; Vomiero, A. High Efficiency Sandwich Structure Luminescent Solar Concentrators Based on Colloidal Quantum Dots. *Nano Energy* **2019**, *60*, 119−126.

(17) Zhao, H.; Liu, G.; Han, G. High-Performance Laminated Luminescent Solar Concentrators Based on Colloidal Carbon Quantum Dots. *Nanoscale Adv.* **2019**, *1*, 4888−4894.

(18) Liu, X.; Luo, B.; Liu, J.; Jing, D.; Benetti, D.; Rosei, F. Eco-Friendly Quantum Dots for Liquid Luminescent Solar Concentrators. *J. Mater. Chem. A* **2020**, *8*, 1787−1798.

(19) Bergren, M. R.; Makarov, N. S.; Ramasamy, K.; Jackson, A.; Guglielmetti, R.; McDaniel, H. High-Performance CuInS2 Quantum Dot Laminated Glass Luminescent Solar Concentrators for Windows. *ACS Energy Lett.* **2018**, *3*, 520−525.

(20) Credi, C.; Pintossi, D.; Bianchi, C. L.; Levi, M.; Griffini, G.; Turri, S. Combining Stereolithography and Replica Molding: On the Way to Superhydrophobic Polymeric Devices for Photovoltaics. *Mater. Des.* **2017**, *133*, 143−153.

(21) Pintossi, D.; Colombo, A.; Levi, M.; Dragonetti, C.; Turri, S.; Griffini, G. UV-Curable Fluoropolymers Crosslinked with Functional Fluorescent Dyes: The Way to Multifunctional Thin-Film Luminescent Solar Concentrators. *J. Mater. Chem. A* **2017**, *5*, 9067−9075.

(22) Tatsi, E.; Fortunato, G.; Rigatelli, B.; Lyu, G.; Turri, S.; Evans, R. C.; Griffini, G. Thermoresponsive Host Polymer Matrix for Self-Healing Luminescent Solar Concentrators. *ACS Appl. Energy Mater.* **2020**, *3*, 1152−1160.

(23) Vauthier, M.; Jierry, L.; Oliveira, J. C.; Hassouna, L.; Roucoules, V.; Bally-Le Gall, F. Interfacial Thermoreversible Chemistry on Functional Coatings: A Focus on the Diels−Alder Reaction. *Adv. Funct. Mater.* **2019**, *29*, No. 1806765.

(24) Binder, W. H. *Self-Healing Polymers: From Principles to Applications*; Wiley-VCH, 2013.

(25) Yang, Y.; Urban, M. W. Self-Healing Polymeric Materials. *Chem. Soc. Rev.* **2013**, *42*, 7446−7467.

(26) Bekas, D. G.; Tsirka, K.; Baltzis, D.; Paipetis, A. S. Self-Healing Materials: A Review of Advances in Materials, Evaluation, Characterization and Monitoring Techniques. *Composites, Part B* **2016**, *87*, 92−119.

(27) van der Zwaag, S. An Introduction to Material Design Principles: Damage Prevention versus Damage Management. In *Self Healing Materials: An Alternative Approach to 20 Centuries of Materials Science*; van der Zwaag, S., Ed.; Springer-Verlag: Berlin, 2007; pp 1−18.

(28) Habault, D.; Zhang, H.; Zhao, Y. Light-Triggered Self-Healing and Shape-Memory Polymers. *Chem. Soc. Rev.* **2013**, *42*, 7244−7256.

(29) Kaur, G.; Johnston, P.; Saito, K. Photo-Reversible Dimerisation Reactions and Their Applications in Polymeric Systems. *Polym. Chem.* **2014**, *5*, 2171−2186.

(30) Frisch, H.; Marschner, D. E.; Goldmann, A. S.; Barner-Kowollik, C. Wavelength-Gated Dynamic Covalent Chemistry. *Angew. Chem., Int. Ed.* **2018**, *57*, 2036−2045.

(31) Trenor, S. R.; Shultz, A. R.; Love, B. J.; Long, T. E. Coumarins in Polymers: From Light Harvesting to Photo-Cross-Linkable Tissue Scaffolds. *Chem. Rev.* **2004**, *104*, 3059−3077.

(32) Lin, H.; Wan, X.; Jiang, X.; Wang, Q.; Yin, J. A "Thiol-Ene" Photo-Curable Hybrid Fluorinated Resist for the High-Performance Replica Mold of Nanoimprint Lithography (NIL). *J. Mater. Chem.* **2012**, *22*, 2616−2623.

(33) Lu, D.; Zhu, M.; Wu, S.; Wang, W.; Lian, Q.; Saunders, B. R. Triply Responsive Coumarin-Based Microgels with Remarkably Large Photo-Switchable Swelling. *Polym. Chem.* **2019**, *10*, 2516−2526.

(34) Marturano, V.; Marcille, H.; Cerruti, P.; Bandeira, N. A. G.; Giamberini, M.; Trojanowska, A.; Tylkowski, B.; Carfagna, C.; Ausanio, G.; Ambrogi, V. Visible-Light Responsive Nanocapsules for Wavelength-Selective Release of Natural Active Agents. *ACS Appl. Nano Mater.* **2019**, *2*, 4499−4506.

(35) Samanta, P.; Kapat, K.; Maiti, S.; Biswas, G.; Dhara, S.; Dhara, D. PH-Labile and Photochemically Cross-Linkable Polymer Vesicles from Coumarin Based Random Copolymer for Cancer Therapy. *J. Colloid Interface Sci.* **2019**, *555*, 132−144.

(36) Ling, J.; Rong, M. Z.; Zhang, M. Q. Coumarin Imparts Repeated Photochemical Remendability to Polyurethane. *J. Mater. Chem.* **2011**, *21*, 18373−18380.

(37) Ling, J.; Rong, M. Z.; Zhang, M. Q. Photo-Stimulated Self-Healing Polyurethane Containing Dihydroxyl Coumarin Derivatives. *Polymer* **2012**, *53*, 2691−2698.

(38) Aguirresarobe, R. H.; Martin, L.; Aramburu, N.; Irusta, L.; Fernandez-Berridi, M. J. Coumarin Based Light Responsive Healable Waterborne Polyurethanes. *Prog. Org. Coat.* **2016**, *99*, 314−321.

(39) Seoane Rivero, R.; Bilbao Solaguren, P.; Gondra Zubieta, K.; Peponi, L.; Marcos-Fernández, A. Synthesis, Kinetics of Photo-Dimerization/Photo-Cleavage and Physical Properties of Coumarin-Containing Branched Polyurethanes Based on Polycaprolactones. *eXPRESS Polym. Lett.* **2016**, *10*, 84−95.

(40) Abdallh, M.; Hearn, M. T. W.; Simon, G. P.; Saito, K. Light Triggered Self-Healing of Polyacrylate Polymers Crosslinked with 7-Methacryloyoxycoumarin Crosslinker. *Polym. Chem.* **2017**, *8*, 5875−5883.

(41) Wang, J. P.; Wang, J. K.; Zhou, Q.; Li, Z.; Han, Y.; Song, Y.; Yang, S.; Song, X.; Qi, T.; Möhwald, H.; Shchukin, D.; Li, G. L. Adaptive Polymeric Coatings with Self-Reporting and Self-Healing Dual Functions from Porous Core−Shell Nanostructures. *Macromol. Mater. Eng.* **2018**, *303*, No. 1700616.

(42) Abdallh, M.; Yoshikawa, C.; Hearn, M. T. W.; Simon, G. P.; Saito, K. Photoreversible Smart Polymers Based on $2\pi + 2\pi$ Cycloaddition Reactions: Nanofilms to Self-Healing Films. *Macromolecules* **2019**, *52*, 2446−2455.

(43) Hughes, T.; Simon, G. P.; Saito, K. Photocuring of 4-Arm Coumarin-Functionalised Monomers to Form Highly Photoreversible Crosslinked Epoxy Coatings. *Polym. Chem.* **2019**, *10*, 2134−2142.

(44) Wang, Y.; Liu, Q.; Li, J.; Ling, L.; Zhang, G.; Sun, R.; Wong, C. P. UV-Triggered Self-Healing Polyurethane with Enhanced Stretchability and Elasticity. *Polymer* **2019**, *172*, 187−195.

(45) Wong, C. S.; Hassan, N. I.; Su'ait, M. S.; Pelach Serra, M. A.; Mendez Gonzalez, J. A.; Granda, L. A.; Badri, K. H. Photo-Activated Self-Healing Bio-Based Polyurethanes. *Ind. Crops Prod.* **2019**, *140*, No. 111613.

(46) Kiskan, B.; Yagci, Y. Self-Healing of Poly(Propylene Oxide)-Polybenzoxazine Thermosets by Photoinduced Coumarine Dimerization. *J. Polym. Sci., Part A: Polym. Chem.* **2014**, *52*, 2911−2918.

(47) Banerjee, S.; Tripathy, R.; Cozzens, D.; Nagy, T.; Keki, S.; Zsuga, M.; Faust, R. Photoinduced Smart, Self-Healing Polymer Sealant for Photovoltaics. *ACS Appl. Mater. Interfaces* **2015**, *7*, 2064−2072.

(48) Owens, D. K.; Wendt, R. C. Estimation of the Surface Free Energy of Polymers. *J. Appl. Polym. Sci.* **1969**, *13*, 1741−1747.

(49) Arnold, R. G.; Nelson, J. A.; Verbanc, J. J. Recent Advances in Isocyanate Chemistry. *Chem. Rev.* **1957**, *57*, 47−76.

(50) Kuş, N.; Breda, S.; Reva, I.; Tasal, E.; Ogretir, C.; Fausto, R. FTIR Spectroscopic and Theoretical Study of the Photochemistry of Matrix-Isolated Coumarin. *Photochem. Photobiol.* **2007**, *83*, 1237−1253.

(51) Abu-Eittah, R.; Moustafa, H.; Al-Omar, A. M. The Electronic Absorption Spectra of Some N-Sulfinylanilines. A Molecular Orbital Treatment. *Can. J. Chem.* **1997**, *75*, 934−941.

(52) Donovalová, J.; Cigáň, M.; Stankovičová, H.; Gašpar, J.; Danko, M.; Gáplovský, A.; Hrdlovič, P. Spectral Properties of Substituted Coumarins in Solution and Polymer Matrices. *Molecules* **2012**, *17*, 3259−3276.

(53) Ling, J.; Rong, M. Z.; Zhang, M. Q. Effect of Molecular Weight of PEG Soft Segments on Photo-Stimulated Self-Healing Performance of Coumarin Functionalized Polyurethanes. *Chin. J. Polym. Sci.* **2014**, *32*, 1286−1297.

(54) Korchia, L.; Bouilhac, C.; Aubert, A.; Robin, J.; Lapinte, V. Light-Switchable Nanoparticles Based on Amphiphilic Diblock, Triblock and Heterograft. *RSC Adv.* **2017**, *7*, 42690−42698.

(55) Trovati, G.; Sanches, E. A.; Neto, S. C.; Mascarenhas, Y. P.; Chierice, G. O. Characterization of Polyurethane Resins by FTIR, TGA, and XRD. *J. Appl. Polym. Sci.* **2010**, *115*, 263−268.

(56) Rosu, D.; Rosu, L.; Cascaval, C. N. IR-Change and Yellowing of Polyurethane as a Result of UV Irradiation. *Polym. Degrad. Stab.* **2009**, *94*, 591−596.

(57) Griffini, G.; Levi, M.; Turri, S. Novel High-Durability Luminescent Solar Concentrators Based on Fluoropolymer Coatings. *Prog. Org. Coat.* **2014**, *77*, 528−536.

(58) Carlotti, M.; Ruggeri, G.; Bellina, F.; Pucci, A. Enhancing Optical Efficiency of Thin-Film Luminescent Solar Concentrators by Combining Energy Transfer and Stacked Design. *J. Lumin.* **2016**, *171*, 215−220.

(59) Babusca, D.; Benchea, A. C.; Dimitriu, D. G.; Dorohoi, D. O. Spectral and Quantum Mechanical Characterization of 3-(2-Benzothiazolyl)-7-(Diethylamino) Coumarin (Coumarin 6) in Binary Solution. *Anal. Lett.* **2017**, *50*, 2740−2754.

(60) Sottile, M.; Tomei, G.; Borsacchi, S.; Martini, F.; Geppi, M.; Ruggeri, G.; Pucci, A. Epoxy Resin Doped with Coumarin 6: Example of Accessible Luminescent Collectors. *Eur. Polym. J.* **2017**, *89*, 23−33.

(61) Griffini, G.; Brambilla, L.; Levi, M.; Del Zoppo, M.; Turri, S. Photo-Degradation of a Perylene-Based Organic Luminescent Solar Concentrator: Molecular Aspects and Device Implications. *Sol. Energy Mater. Sol. Cells* **2013**, *111*, 41−48.

(62) Rechthaler, K.; Köhler, G. Excited State Properties and Deactivation Pathways of 7-Aminocoumarins. *Chem. Phys.* **1994**, *189*, 99−116.

(63) Wu, W.; Cao, Z.; Zhao, Y. Theoretical Studies on Absorption, Emission, and Resonance Raman Spectra of Coumarin 343 Isomers. *J. Chem. Phys.* **2012**, *136*, No. 114305.

(64) Berney, C.; Danuser, G. FRET or No FRET: A Quantitative Comparison. *Biophys. J.* **2003**, *84*, 3992−4010.

(65) Clapp, A. R.; Medintz, I. L.; Mauro, J. M.; Fisher, B. R.; Bawendi, M. G.; Mattoussi, H. Fluorescence Resonance Energy Transfer between Quantum Dot Donors and Dye-Labeled Protein Acceptors. *J. Am. Chem. Soc.* **2004**, *126*, 301−310.

(66) Bailey, S. T.; Lokey, G. E.; Hanes, M. S.; Shearer, J. D. M.; McLafferty, J. B.; Beaumont, G. T.; Baseler, T. T.; Layhue, J. M.; Broussard, D. R.; Zhang, Y. Z.; Wittmershaus, B. P. Optimized Excitation Energy Transfer in a Three-Dye Luminescent Solar Concentrator. *Sol. Energy Mater. Sol. Cells* **2007**, *91*, 67−75.

(67) Lakowicz, J. R. Energy Transfer. In *Principles of Fluorescence Spectroscopy*; Springer Science & Business Media, 2013; pp 368−394.

(68) Lyu, G.; Kendall, J.; Meazzini, I.; Preis, E.; Bayseç, S.; Scherf, U.; Clément, S.; Evans, R. C. Luminescent Solar Concentrators Based on Energy Transfer from an Aggregation-Induced Emitter Conjugated Polymer. *ACS Appl. Polym. Mater.* **2019**, *1*, 3039−3047.

(69) Balaban, B.; Doshay, S.; Osborn, M.; Rodriguez, Y.; Carter, S. A. The Role of FRET in Solar Concentrator Efficiency and Color Tunability. *J. Lumin.* **2014**, *146*, 256−262.

(70) Al-Kaysi, R. O.; Sang Ahn, T.; Müller, A. M.; Bardeen, C. J. The Photophysical Properties of Chromophores at High (100 MM and above) Concentrations in Polymers and as Neat Solids. *Phys. Chem. Chem. Phys.* **2006**, *8*, 3453−3459.

(71) Haines, C.; Chen, M.; Ghiggino, K. P. The Effect of Perylene Diimide Aggregation on the Light Collection Efficiency of Luminescent Concentrators. *Sol. Energy Mater. Sol. Cells* **2012**, *105*, 287−292.

(72) Yoo, H.; Yang, J.; Yousef, A.; Wasielewski, M. R.; Kim, D. Excimer Formation Dynamics of Intramolecular π-Stacked Perylenediimides Probed by Single-Molecule Fluorescence Spectroscopy. *J. Am. Chem. Soc.* **2010**, *132*, 3939−3944.

(73) Banal, J. L.; White, J. M.; Lam, T. W.; Blakers, A. W.; Ghiggino, K. P.; Wong, W. W. H. A Transparent Planar Concentrator Using Aggregates of Gem-Pyrene Ethenes. *Adv. Energy Mater.* **2015**, *5*, No. 1500818.

(74) Banal, J. L.; Soleimaninejad, H.; Jradi, F. M.; Liu, M.; White, J. M.; Blakers, A. W.; Cooper, M. W.; Jones, D. J.; Ghiggino, K. P.; Marder, S. R.; Smith, T. A.; Wong, W. W. H. Energy Migration in Organic Solar Concentrators with a Molecularly Insulated Perylene Diimide. *J. Phys. Chem. C* **2016**, *120*, 12952−12958.